Extension of Computational Chemistry to the Study of Lanthanide(III) Ions in Aqueous Solution: Implementation and Validation of a Continuum Solvent Approach

U. Cosentino, A. Villa,* and D. Pitea

Dipartimento di Scienze dell'Ambiente e del Territorio, Università degli Studi di Milano-Bicocca, P.zza della Scienza 1, 20126 Milano, Italy

G. Moro

Dipartimento di Biotecnologie e Bioscienze, Università degli Studi di Milano-Bicocca, P.zza della Scienza 2, 20126 Milano, Italy

V. Barone

Dipartimento di Chimica, Università Federico II, via Mezzocannone 4, 80134 Napoli, Italy

Received: November 12, 1999; In Final Form: June 13, 2000

A set of atomic radii used for the construction of solute cavities in the framework of the polarizable continuum model (PCM) is extended and validated with the aim of supporting the investigation of lanthanide(III) complexes in aqueous solution. The parameterization of the atomic radii for the whole Ln(III) series is performed by minimizing the differences between the experimental and the calculated standard hydration free energies of the ions calculated at the HF level. The optimized radii show a remarkable linear relationship with effective ionic radii and well reproduce the experimental hydration free energies also when electron correlation effects are included in the calculations. We have next validated a mixed discrete continuum model in which a supermolecule formed by the ion and by water molecules in the first hydration shell is immersed in a polarizable continuum. The molecular structures, the relative stability of the octa- with respect to the nonahydrated species, and the ion hydration free energies have been calculated for the neodymium(III) and ytterbium(III) aqueous ions. Results are in agreement with experimental evidence, both from structural and energetic standpoints. The molecular structures optimized including surrounding effects are in better agreement with the experimental structures than the in vacuo geometries. Moreover, the results show that the energetic properties of these systems in aqueous solution can be effectively calculated by using the structures optimized in vacuo, and including correlation effects in the gas-phase reaction of complex formation.

Introduction

In recent years there has been a particular interest in the investigation of complexes of trivalent lanthanide ions, Ln(III). Due to the paramagnetic properties of Ln(III) ions, their complexes are employed as contrast agents in magnetic resonance imaging (MRI) diagnostic techniques and as shift reagents in NMR analysis of electrolytes in biological tissues.[1] As the free lanthanide ions are very toxic, complexes with polydentate ligands presenting high kinetic and thermodynamic stability in solution are used as MRI contrast agents. Frequently, one or more water molecules are coordinated to the ion in these complexes; this fact is particularly relevant for the use of these complexes as MRI contrast agents, as the ability of the complex to enhance the image contrast is related to its relaxivity, that is, the efficiency to increase the relaxation rate of the water protons via dipolar interactions. Thus, among other factors, relaxivity is affected by the chemical exchange between water molecules in the first solvation shell and the bulk solvent.

Theoretical investigation of these complexes can represent a valid tool to study their structures and dynamics and to identify the relevant factors that make these complexes useful in diagnostic applications. A reliable computational approach may be particularly suitable for gadolinium complexes, since the high magnetic moment of the ion precludes the use of the usual experimental techniques, such as NMR spectroscopy. In fact, gadolinium aqueous ion[2] and gadolinium complexes with polyamino carboxylate ligands[3] were previously investigated in vacuo by means of ab initio methods.

However, an accurate and realistic modeling of these systems requires the investigation of their behavior in solution and, thus, must include surrounding effects. The continuum approach[4] offers a simple methodology for including solvent effect in the study of complex systems. Among the methods developed up to now, the polarizable continuum model (PCM)[5] offers a balanced and theoretically sound treatment of all solute−solvent interactions at a very reasonable computational cost.

One of the main factors affecting the accuracy of continuum solvent models is the use of properly tailored solute cavities. Several cavity definitions are reported[4] in the literature; among these, we have selected the united atom topological model (UATM),[6] in which the whole cavity is the envelope of spheres centered on atoms or atomic groups with radii based on classical chemical concepts such as hybridation and formal charge. As a matter of fact, while UATM radii are close to standard van der

* To whom correspondence should be addressed: Dr. Alessandra Villa, Dipartimento di Chimica Fisica ed Elettrochimica, Università degli Studi di Milano, Via Golgi 19, 20133 Milano, Italy. Phone ++39 02 26603247; Fax ++39 02 70638129; E-mail: a.villa@csrsrc.mi.cnr.it.

10.1021/jp994022n CCC: $19.00
Published on Web 07/26/2000

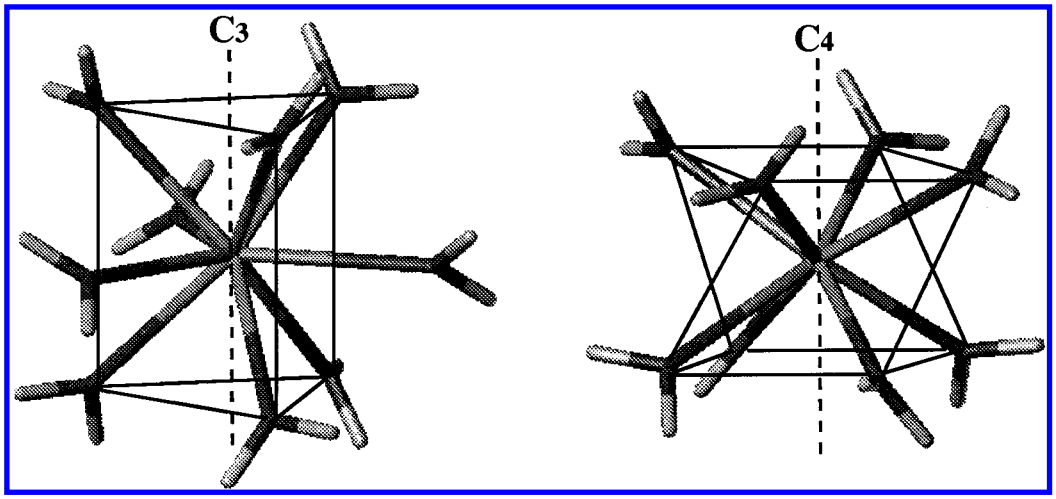

Figure 1. TCTP (D_3) and SQA (S_8) coordination geometries of the $[Nd(H_2O)_9]^{3+}$ and $[Yb((H_2O)_8]^{3+}$ in vacuo optimized structures.

Waals or ionic radii, several studies have shown that fine-tuning of radii is essential for reliable computations of solvation energies and solvent shifts on the structural and spectroscopic properties of the solute. The remarkable results obtained for both neutral and charged solutes formed by main group atoms prompted us to extend the UATM model to the lanthanide ions.

In recent years, the solvation of several metal ions has been studied by ab initio quantum mechanical computations in which the first hydration shell is described by means of a proper cluster of water molecules, while interactions with the bulk are simulated by a discrete second shell[7] or by a continuum solvent.[8] On the other hand, the solvation of lanthanide ions has been investigated only by Monte Carlo and molecular dynamics simulations employing classical pair potentials in conjunction with unpolarizable[9] or polarizable[10] water molecule models.

To extend the possibility of studying Ln(III) complexes in condensed phases at the ab initio level by means of the PCM, the parameterization of the atomic radii used within the UATM scheme for the whole Ln(III) series is reported in this paper. Furthermore, due to the relevance of the ion-coordinated water molecules, the reliability of PCM/UATM in determining coordination numbers (CN) and hydration free energies of Ln(III) aqueous ions was tested by using a mixed model in which a cluster formed by the ion and by the water molecules belonging to the first hydration shell is immersed in a polarizable continuum.

For lanthanides, crystallographic structures of the aqueous ions with different counterions (ethyl sulfate,[11] triflate,[12] and bromate[13]) as well as experimental evidence on structures and dynamics in solution[14] are available. In the solid state, all of the lanthanides are 9-coordinated and present a tricapped trigonal prism (TCTP) geometry around the ion (Figure 1). In the ideal TCTP geometry there are six equivalent positions (axial oxygens, O_{ax}) at the vertices of a regular trigonal prism and three equivalent positions (equatorial oxygens, O_{eq}) that cap the rectangular faces of the prism. Although the coordination geometry of all nonaqueous ions is similar, there are counterion dependent structural differences: ethyl sulfate[11] and triflate[12] aqueous ions show C_{3h} symmetry, while bromate aqueous ions present[13] D_{3h} symmetry. Ab initio calculations on the $[Gd(H_2O)_9]^{3+}$ system showed that[2] in vacuo this system has only one minimum energy conformation, presenting a TCTP coordination geometry with D_3 symmetry. Neutron diffraction experiments on lanthanide solutions[14b] reveal that from La to Nd the ions are 9-hydrated, with a TCTP coordination geometry, whereas from Gd to Lu they are 8-hydrated, with structures consistent with a square antiprismatic (SQA) coordination geometry (Figure 1).

To analyze the different behavior of lanthanide ions in solution, the neodymium(III) and ytterbium(III) aquo ions have been here investigated.

Methods

Sovaltion Free Energy Calculation. The dominant contribution to the variation of free energy when going from vacuo to solution, i.e., the solvation free energy (ΔG_{sol}), is the work spent in transferring the solute from a fixed position in the ideal gas phase to a fixed position in the liquid phase (W_o). However, for polyatomic solutes also the energy variation related to the structural and vibrational modification of the solute induced by the solvent must be taken into account. Following previous studies,[4,5] we will assume that the translational and rotational solute partition functions are identical in vacuo and in solution (i.e., the solute has a very large volume available in the solvent and it can rotate freely). The work spent in modifying the structure of the isolated solute to its most stable structure in solution is referred to in the following as W_{geom}. Note that this term includes also the thermal contribution deriving from the variation of the rotational partition function issuing from geometry variations. The contribution issuing from the modifications of the zero point energy, ZPE, and of the vibrational solute partition function, referred to the ground vibrational level and calculated in the harmonic approximation, when going from vacuo to solution is referred to in the following as W_{vib}. In summary, ΔG_{sol} can be written:

$$\Delta G_{sol} = W_o + W_{geom} + W_{vib} \quad (1)$$

In the PCM, W_o is defined as the work required to build the solute cavity in the solvent (cavitation energy, W_{cav}) together with the electrostatic (W_{el}) and nonelectrostatic work ($W_{disp} + W_{rep}$) connected with charging the solute and switching the solute−solvent interactions on:

$$W_o = W_{el} + W_{cav} + W_{disp} + W_{rep} \quad (2)$$

Finally, the total free energy of a species in solution (G_{sol}) is evaluated by adding ΔG_{sol} to the free energy of the species in vacuo (G_{vac}). This last term corresponds to the sum of the electronic energy (E_{el}) and the nonpotential energy (NPE) contributions (that is, the ZPE and the thermal terms), collectively referred to as G_{NPE}.

$$G_{sol} = G_{vac} + \Delta G_{sol} = E_{el} + G_{NPE} + \Delta G_{sol} \quad (3)$$

In our calculations, G_{vac} and G_{sol} refer to the minimum energy conformation calculated in vacuo and in solution, respectively.

Computational Details. Calculations were performed using for the ions the quasi relativistic effective core potentials (ECPs), that include 46 + 4f^n electrons in the core (1s−4d, 4f^n), and the related [5s4p3d]-GTO valence basis sets.[15] The reliability of these ECPs has been previously investigated by in vacuo calculations on different Gd systems.[2,3] For the water molecules, the 6-31G* basis set was used: previous investigation of the $[Gd(H_2O)_9]^{3+}$ aqueous ion showed that[2] geometries and conformational energies are not significantly affected by using more extended basis sets (6-31G**, D95**).

Inclusion of solvent effect was performed using our implementation of the COSMO model,[16] here referred to as conductor-like PCM, C−PCM,[17] due to the fact that analytical second derivatives are available only for this implementation.[18] In any case, C−PCM and the conventional dielectric-like PCM (D-PCM) provide essentially the same results in polar solvents.[5] The UATM procedure was used to build the solute cavity; for the water molecules, the standard D-PCM/UATM radius (1.68 Å) was used. In fact, reoptimization of the water radius in C−PCM provided the same value obtained by conventional D-PCM.

In all of the calculations, lanthanide dispersion and repulsion parameters were set to zero, due to their negligible influence in highly charged ions. As usual,[6] all of the UATM radii (of water and lanthanides) were scaled by 1.2 factor in the calculations of electrostatic contributions, while the unscaled values were used for calculation of the other contributions. A modified version of the Gaussian 98 package,[19] including second derivatives for C−PCM, was used.

For the $[Ln(H_2O)_8]^{3+}$ and the $[Ln(H_2O)_9]^{3+}$ species of the Nd and Yb ions, in the following referred to as (Ln-**8**) and (Ln-**9**), full geometry optimizations at the HF level followed by frequency analysis were performed both in vacuo and in aqueous solution.[20] On the in vacuo optimized geometries, further single point calculations were performed at the MP2 level, neglecting correlation involving the inner shell 1s electrons of oxygen atoms, and using the hybrid density functional model mPW1PW.[21] Calculations in solution were performed using an average area of 0.4 Å^2 for all the finite elements (tesserae) used to build the solute cavities, and removing the linear search in the Berny algorithm used for geometry optimizations. As C−PCM analytical second derivatives are available only for the electrostatic contribution, the cavitation, dispersion, and repulsion contributions to W_o were omitted in geometry optimizations as well as in the frequency analyses performed on the optimized structures. The final energies obtained from single point calculations at optimized geometries in solution include both electrostatic and nonelectrostatic contributions.

In vacuo optimizations started for the (Ln-**8**) species from a SQA coordination polyhedron, with (C_4) and without (C_1) symmetry; for (Ln-**9**) optimizations started from the C_{3h} and D_{3h} TCTP arrangements observed in the crystallographic structures and from the previously calculated[2] D_3 structure of $[Gd(H_2O)_9]^{3+}$. In solution, optimizations of both the species were performed starting from the corresponding in vacuo minima, relaxing symmetry constraints because they are not supported in the actual implementation of PCM in Gaussian 98.

TABLE 1. UATM[a] and Ionic Radii (Å) for Lanthanide (III) Ions, Together with Experimental and HF, MP2, and DFT Calculated Standard Hydration Free Energies (ΔG°_{hyd}, kcal mol^{-1})

	UATM radii	ionic radii[27]	ΔG°_{hyd} exp[b]	HF	MP2	mPW1PW
La	1.550	1.216	−788.1	−790.4	−790.6	−790.3
Ce	1.523	1.196	−802.4	−804.6	−804.7	−804.5
Pr	1.513	1.179	−810.1	−812.5	−812.3	−812.5
Nd	1.497	1.163	−816.5	−818.6	−818.8	−818.5
Sm	1.467	1.132	−833.5	−835.4	−835.6	−835.4
Eu	1.461	1.120	−841.1	−838.8	−839.0	−838.7
Gd	1.447	1.107	−845.2	−847.0	−847.2	−846.9
Tb	1.438	1.095	−850.5	−852.3	−852.4	−852.3
Dy	1.423	1.083	−859.9	−861.3	−861.5	−861.3
Ho	1.418	1.072	−862.7	−864.3	−864.5	−864.3
Er	1.411	1.062	−867.4	−868.6	−868.8	−868.6
Tm	1.395	1.052	−877.3	−878.7	−878.8	−878.7
Yb	1.384	1.042	−884.1	−885.7	−885.8	−885.7
Lu	1.378	1.032	−888.1	−889.5	−889.6	−889.5

[a] To be scaled by 1.2 factor in the calculations of electrostatic contributions. [b] See note 22.

Results and Discussion

UATM Lanthanide(III) Atomic Radii Parameterization. The UATM lanthanide atomic radii were determined by minimizing the differences between the experimental (see note 22) and the HF-calculated standard hydration free energies of lanthanide(III) ions at 298.15 K. The standard hydration free energy for the reaction

$$Ln^{3+}(g) \rightarrow Ln^{3+}(sol) \quad (4)$$

is calculated according to

$$\Delta G^\circ_{hyd} = \Delta G_{sol} + RT \ln(M_{sol}/M_g) \quad (5)$$

where ΔG_{sol} is the solvation free energy computed by eq 1, R is the gas constant, and T the absolute temperature. The second term in the right hand side of eq 5 is due to the different standard concentrations of solution (M_{sol}) and gas phase ($M_g = P/RT$). The value of the $RT\ln(M_{sol}RT/P)$ term is 1.87 kcal mol^{-1} for T = 298.15 (K), P = 1 (atm), and M_{sol} = 1 (M).

The UATM radii derived at the HF level together with the experimental and the HF, MP2, and DFT calculated ΔG°_{hyd} values for the whole lanthanide series are reported in Table 1. The reliability of the UATM radii (R_{UATM}) is strongly supported by the observed linear relationship between R_{UATM} and the lanthanide ionic radii[27] (R_{ion}) (Figure 2). Ordinary least-squares analysis provides (R^2 = 0.997)

$$R_{UATM} = 0.439 + 0.911\, R_{ion} \quad (6)$$

According to eq 6, the UATM radii decrease along the series. This reflects the experimental evidence that heavier lanthanides present stronger interactions with water. Moreover, the linear relationship of eq 6 is of particular relevance within the UATM framework. In fact, in the case of ions, the most natural choice for the UATM radii should derive from a linear relationship with ionic radii. Indeed, the solvation free energies computed by means of the PCM using the UATM radii calculated by eq 6 are in excellent agreement with the experimental values (Figure 3). Furthermore, test computations showed that essentially the same optimized radii are obtained by using conventional D-PCM. Finally, the remarkable agreement of MP2 and DFT ΔG°_{hyd} values, calculated with the HF implemented radii, with the HF results shows that in the case of highly

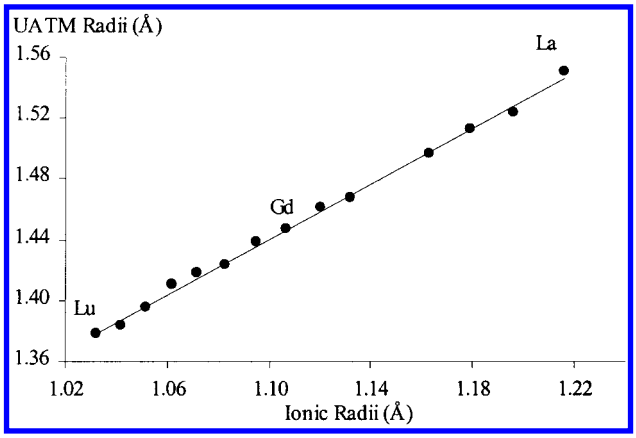

Figure 2. Lanthanide UATM radii versus ionic radii and the linear regression model of eq 6.

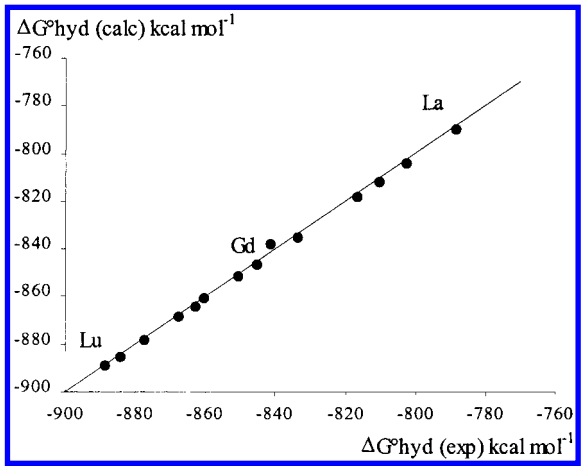

Figure 3. Standard hydration free energies calculated using the UATM radii derived from eq 6 versus the experimental values.

charged ions the parameterization at the HF level permits to derive well calibrated radii that can also be used confidently for calculations at higher theory levels. These results give further support both on the physical soundness of the continuum solvent model and on the general philosophy underlying the building of the solute cavities. Of course, some specific solvent molecules should be included in the computation for such charged species in polar solvents (see next paragraph) but the availability of the metal radii allows the building of a general purpose model that can be used for different situations.

Calculations on Lanthanide Aqueous Ions. The reliability of the PCM using the UATM cavity definition to study water molecules coordinated to highly positive charged ions was tested. In the following, we report the results obtained using a mixed model in which the water molecules belonging to the first hydration shell are considered while the bulk water molecules are described by means of PCM. The investigation on Nd and Yb aqueous ions concerns molecular structures, relative stability of the octa- with respect to the nonahydrated species, and ion hydration free energies.

Molecular Geometries. The results of the geometry optimizations of the octa- and nona-coordinated Nd and Yb systems performed both in vacuo and in solution are reported in Table 2, together with the experimental data. Full geometry optimizations followed by frequency analysis provide (Figure 1) an SQA minimum energy structure for the (Ln-**8**) species and a TCTP arrangement for the (Ln-**9**) species, both in vacuo and in solution (see note 28). The calculated structures for the (Ln-**9**) species correctly reproduce the TCTP coordination geometry observed in the crystallographic structures of Nd and Yb systems,[11,12] and in the structure determined in solution for Nd aqueous ion.[14b,d] Moreover, the SQA arrangement computed for the most stable structure of the $[Yb(H_2O)_8]^{3+}$ system in solution is consistent with the results of neutron diffraction experiments.[14b]

The Ln−O bond lengths computed in vacuo are always longer than the experimental ones; in-solution results provide a better agreement with the experimental data. The shortening of the Ln−O bond distances observed in solution can be ascribed to a stronger water−ion interaction due to the solvent polarization effects that, increasing the dipole moment of the free water molecules, increase the water−ion interaction. In fact, it is well known that the experimental dipole moment of one water molecule increases passing from vacuum ($\mu = 1.85$ D) to water solution ($\mu = 2.60$ D).[29] This trend is also reproduced by C−PCM calculations at the HF/6-31G* level ($\mu = 2.20$ and 2.47 D in vacuo and solution, respectively), even if more sophisticated methods and basis sets should be required to reproduce the experimental values. As a further support, increasing the polarity of O−H bonds in the coordinated water molecules in solution with respect to vacuum can be highlighted from the absolute values of Mulliken charges for oxygens and hydrogens obtained in solution (on average 2% larger than in vacuo). These results underline the importance of a proper inclusion of surrounding effects in the investigation of the structural properties of these systems in condensed phases.

Relative Stabilities. The relative stabilities of the octahydrated species (Ln-**8**) with respect to the nonahydrated species (Ln-**9**) for the Nd and Yb aqueous ions in solution were determined by calculating the free energy variation (ΔG_{react}) for the reaction by

$$[Ln(H_2O)_8]^{3+}(sol) + H_2O(sol) \rightarrow [Ln(H_2O)_9]^{3+}(sol) \quad (7)$$

In other words, the binding free energy of one water molecule to the (Ln-**8**) species

$$\Delta G_{react} = G_{sol}(\text{Ln-}\mathbf{9}) - G_{sol}(\text{Ln-}\mathbf{8}) - G_{sol}(\mathbf{wat}) \quad (8)$$

Table 3 reports the free energy variations ΔG_{react} defined in eq 8 for the Nd and Yb aqueous ions together with the free energies in solution (G_{sol}) for each species involved in reaction 7. According to equations 1 and 3, all of the contributions to the free energies and to the free energy variations are also reported. The ΔG_{react} values (negative in the case of Nd and positive in the case of Yb) are in agreement with the experimental evidence[14] that the Nd aqueous ion is nona-coordinated and the Yb aquo ion is octa-coordinated.

To better analyze the energetic aspects involved in reaction 7, first we will discuss the contributions to ΔG_{react} from in vacuo reaction, then those due to the solvent effects. In vacuo, the main difference between Nd and Yb systems lies in the variation of the electronic energy (ΔE_{el}) associated to reaction 7 (Table 3): both values are negative, but Nd presents the most favorable interaction energy (−27.7 versus −23.2 kcal mol^{-1}). The ΔG_{NPE} contribution to reaction 7 is around 12 kcal mol^{-1} for both ions and it is mainly due to the free energy variation associated with the loss of the rotational (−2.2 kcal mol^{-1}) and translational (−8.8 kcal mol^{-1}) degrees of freedom of the water molecule upon coordination. The remaining part derives from the differences in the rotational (0.1 kcal mol^{-1}) and vibrational (1.5 and 1.0 kcal mol^{-1} for Nd and Yb, respectively) contributions of (Ln-**8**) and (Ln-**9**). Thus the overall free energy variations have negative values in vacuo: −15.1 kcal mol^{-1} in the case of Nd and −11.1 kcal mol^{-1} in the case of Yb. This highlights the

TABLE 2: Geometrical Parameters[a] (Experimental and Calculated In Vacuo and In Solution) of the Coordination Polyhedron for the Investigated Lanthanide Aquo Ions (Ln = Nd, Yb)

	calcd				exp		
	in vacuo	in solution	in vacuo	in solution	X-ray dif.[11] solid state	EXAFS[14d] in solution	neutron dif.[14b] in solution
				Nd			
CN	8	8	9	9	9	9.5	8.9
CG	SQA	SQA	TCTP	TCTP	TCTP	TCTP	TCTP
symmetry	S_8	C_1	D_3	C_1	C_{3h}		
Nd−O_{eq}			2.610		2.570		
Nd−O_{ax}			2.594		2.457		
Nd−O	2.561	2.517		2.558		2.51	2.50
		(0.003)		(0.009)			
φ [b]	57.2	58.1 (0.6)	44.0	45.0 (1.2)	45.1		
θ [c]	45.0	43.8 (0.7)	60.0	60.0 (1.0)	54.3		
				Yb			
CN	8	8	9	9	9		7.8
coord. geometry	SQA	SQA	TCTP	TCTP	TCTP		
symmetry	S_8	C_1	D_3	C_1	C_{3h}		
Yb−O_{eq}			2.509		2.503		
Yb−O_{ax}			2.447		2.324		
Yb−O	2.417	2.373		2.427			2.32
		(0.004)		(0.004)			
φ[b]	57.4	57.7 (0.4)	44.4	45.4 (0.7)	45.3		
θ[c]	45.0	44.0 (0.3)	60.0	60.2 (0.6)	54.9		

[a] Distances (Å), angles (°). Coordination number (CN), coordination geometry (CG), and symmetry are reported. For experimental and in vacuo calculated TCTP geometries, the axial and equatorial Ln−O bond distances are reported; in the other cases, the average (standard deviation). [b] Angle the metal−prism bonds make to the C_3 (TCTP) or to the C_4 (SQA) symmetry axes. [c] Twist angle of the three equatorial oxygens relative to the axial oxygens in the TCTP geometry, or between the upper and lower oxygens in the SQA arrangement.

TABLE 3: Free Energy Variations ΔG_{react} for Reaction 7 together with the Free Energies in Solution (G_{sol}) for Each Involved Species[a]

	ΔG_{react}	G_{sol}[b]	E_{el}[b]	G_{NPE}	W_o	W_{geom}	W_{vib}
			Nd				
(Nd-**9**)		−717.0716	−716.6596	119.4	−365.4	−3.5	−9.0
wat		−76.0163	−76.0107	3.4	−6.3	−0.1	−0.5
(Nd-**8**)		−641.0535	−640.6046	103.4	−372.1	−3.5	−9.5
(Nd-**8**) + **wat** → (Nd-**9**)	−1.1	−1.1[c]	−27.7[c]	12.6	13.0	0.0	1.0
			Yb				
(Yb-**9**)		−722.9872	−722.5629	122.2	−376.4	−3.7	−8.4
wat		−76.0163	−76.0107	3.4	−6.3	−0.1	−0.5
(Yb-**8**)		−646.9736	−646.5151	106.7	−384.5	−2.8	−7.0
(Yb-**8**) + **wat** → (Yb-**9**)	1.7	1.7[c]	−23.2[c]	12.1	14.5	−0.8	−0.9

[a] According to equations 1 and 3, all of the contributions to free energies and free energy variations are reported. Each contribution to ΔG_{react} is calculated according to: $\Delta X = X(\text{Ln-}\mathbf{9}) - X(\text{Ln-}\mathbf{8}) - X(\mathbf{wat})$. [b] G_{sol} and E_{el} in Hartree; the other quantities in kcal mol^{-1}. [c] In kcal mol^{-1}.

tendency of the ninth water molecule to coordinate the ions in vacuo, and this reaction is more favorable for Nd than for Yb.

The main contribution due to the solvent effect (Table 3) is in the W_o term of eq 1. This term assumes positive values for both the ions, underlining that the binding of the ninth water molecule to the octa-coordinated species is an unfavorable process. The inclusion of this term in ΔG_{react} plays a crucial role in determining the correct relative stability of the octa- and nonahydrated species. The other terms related to solvent effects (W_{geom} and W_{vib}) provide smaller contributions and can be neglected without significantly affecting the calculated relative stability of the octa- and nonahydrated species. Therefore, these results suggest that the relative stability of different species in solution can be confidently evaluated using structures optimized in vacuo, skipping the onerous task of geometry optimization and frequency analysis in solution.

Standard Hydration Free Energies. As a further test of the PCM/UATM reliability, the standard hydration free energies of the Nd^{3+} and Yb^{3+} ions were calculated within the framework of the mixed solvation model. In this framework, the standard hydration free energy ($\Delta G°_{hyd}$) corresponds to the free energy variation (ΔG_{react}) of the following reaction:

$$Ln^{3+}(g) + nH_2O(sol) \rightarrow [Ln(H_2O)_n]^{3+}(sol) \quad (9)$$

where n is the number of water molecules considered in the first hydration shell. According to the experimental evidence and to the previously discussed results, the (Nd-**9**) and the (Yb-**8**) species have been considered, respectively, in reaction 9.

To compute the free energy variation involved in reaction 9, the process can be broken down into the following steps:[8b]

$$nH_2O(sol) \rightarrow nH_2O(g) \quad (10)$$

$$Ln^{3+}(g) + nH_2O(g) \rightarrow [Ln(H_2O)_n]^{3+}(g) \quad (11)$$

$$[Ln(H_2O)_n]^{3+}(g) \rightarrow [Ln(H_2O)_n]^{3+}(sol) \quad (12)$$

Therefore, the hydration free energy $\Delta G°_{hyd}$ for reaction 9 consists of the free energy variations associated with evaporation of n water molecules ($\Delta G°_{vap}$) (10), gas-phase complexation ($\Delta G°_{com}$) (11), and complex solvation ($\Delta G°_{com-sol}$) (12):

$$\Delta G°_{hyd} = n\Delta G°_{vap} + \Delta G°_{com} + \Delta G°_{com-sol} \quad (13)$$

TABLE 4: PCM Calculated and Experimental[a] ΔG°_{hyd} Values together with the ΔG°_{vap}, ΔG°_{com},[b] and $\Delta G^\circ_{com-Sol}$ Values (kcal mol^{-1})

	Nd	Yb
CN = n	9	8
$n\,\Delta G^\circ_{vap}$ (HF)	23.4	20.8
ΔG°_{com} (E_{el-HF})	−425.5	−464.2
ΔG°_{com} (E_{el-MP2})	−474.7	−513.6
ΔG°_{com} ($E_{el-mPW1PW}$)	−465.6	−504.9
$\Delta G^\circ_{com-sol}$ (HF)	−376.1	−392.5
ΔG°_{hyd-HF}	−778.2	−835.9
$\Delta G^\circ_{hyd-MP2}$	−827.4	−885.3
$\Delta G^\circ_{hyd-mPW1PW}$	−818.3	−876.6
ΔG°_{hyd} (exp)	−816.5	−884.1

[a] See note 22. [b] Electronic contributions E_{el} to ΔG°_{com} calculated at the HF, MP2, and DFT levels on HF optimized geometries; non potential energy contributions, G_{NPE}, derived from HF calculations.

Here, ΔG°_{vap} and $\Delta G^\circ_{com-sol}$ include the corrective term $RT\ln(M_{sol}/M_g)$ (see eq 5) due to the different standard concentrations of gas phase (P/RT) and solutions (55.5 M for the water; 1 M for the complex).

For the gas-phase complexation (11), the electronic contributions, E_{el}, to ΔG°_{com} have been calculated on the HF optimized structures at the HF, MP2, and DFT levels; non potential energy contributions, G_{NPE}, derive from HF results. The ΔG°_{hyd} calculated values together with the ΔG°_{vap}, ΔG°_{com}, and $\Delta G^\circ_{com-sol}$ contributions for the (Nd-**9**) and the (Yb-**8**) systems are reported in Table 4.

Comparison with the experimental data shows that the hydration free energies of the Nd^{3+} and Yb^{3+} ions are fairly well reproduced at the HF level, even if the experimental values are underestimated by approximately 5% (the errors per water molecule amount to 4.2 and to 6.0 kcal mol^{-1} for Nd and Yb, respectively). The W_{geom} and W_{vib} terms involved in eqs 10 and 12, i.e., all of the contributions related to the geometry relaxation passing from vacuo to solution, amount to 7.2 and to 5.6 kcal mol^{-1} for Nd and Yb, respectively. Thus their omission causes only a slight increase in the errors per water molecule. These results, together with those reported above for relative stability calculations, suggest that the energetics of these systems in solution can be calculated using structures optimized in vacuo, because the contributions due to the geometry relaxation are usually negligible. Moreover, to investigate the possible sources of errors involved in the calculations on reaction 9, we analyzed the effects of electron correlation on the gas phase complexation (eq 11) and on the complex solvation (eq 12) steps. Inclusion of electron correlation in the gas phase complexation by means of MP2 or DFT methods dramatically improves the quality of results (Table 4). On the contrary, the HF results for the solvation of these complexes are not significantly affected by inclusion of the electronic correlation: MP2 and DFT solvation free energies calculated on the HF optimized geometries differ from HF results by less than 0.7 and 0.2 kcal mol^{-1}, respectively. In conclusion, these results show that to achieve a reliable modeling of process (eq 9) in vacuo, high quality calculations are required.

Conclusions

The UATM atomic radii for the whole Ln(III) series implemented at the HF level accurately reproduce the experimental solvation free energies when electron correlation effects are also included in the calculations. Thus, radii reparameterization is not required for highly charged ions when in-solution calculations are performed at theory levels higher than HF.

Results on aqueous ions show that the cavity can be confidently built using the standard water UATM radius, even if it was originally parameterized for bulk water molecules. Moreover, they show that surrounding effects should be included in geometry optimization to obtain molecular structures in better agreement with solid state and solution experimental structures. On the other hand, the energetics of these systems can be appropriately calculated on in vacuo optimized structures, the terms due to the geometry relaxation in solution being negligible. Moreover, it has been shown that correlation effects in the gas-phase complexation reaction are relevant in determining correct hydration free energies, while they do not play any significant role in the aqueous ion solvation.

Finally, all of these results should be considered within the limit of the continuum solvent approach, in which only average solute−solvent effects are included. The inclusion of the first solvation sphere should reduce this source of error, even if this mixed model does not take the dynamic behavior of the coordinated water molecules into account. However, a static model for the first shell can be justified by the presence of a highly charged ion that strongly coordinates the water molecules.

Acknowledgment. Financial support from the Italian National Research Council (CNR Target Project on Biotechnology, Grant n.97.01081.PF49) is gratefully acknowledged.

References and Notes

(1) (a) Caravan, P.; Ellison, J. J.; McMurry, T. J.; Lauffer, R. B. *Chem. Rev.* **1999**, *99*, 2293. (b) Aime, S.; Botta, M.; Fasano, M.; Terreno, E. *Chem. Soc. Rev.* **1998**, *27*, 19.

(2) Cosentino, U.; Moro, G.; Pitea, D.; Calabi, L.; Maiocchi, A. *J. Mol. Struct. THEOCHEM* **1997**, *392*, 75.

(3) Cosentino, U.; Moro, G.; Pitea, D.; Villa, A.; Fantucci, P. C.; Maiocchi, A.; Uggeri, F. *J. Phys. Chem. A* **1998**, *102*, 4606.

(4) Tomasi, J.; Persico, M. *Chem. Rev.* **1994**, *94*, 2027.

(5) Amovilli, C.; Barone, V.; Cammi, R.; Cances, E.; Cossi, M.; Mennucci, B.; Pomelli, C. S.; Tomasi, J. *Adv. Quantum Chem.* **1998**, *32*, 227.

(6) Barone, V.; Cossi, M.; Tomasi, J. *J. Chem. Phys.* **1997**, *107*, 3210.

(7) Pavlov, M.; Siegbhan, P. E. M.; Sandström, M. *J. Phys. Chem. A* **1998**, *102*, 219.

(8) (a) Martinez, J. M.; Pappalardo, R. R.; Sanchez-Marcos, E. *J. Phys. Chem. A* **1996**, *100*, 11748. (b) Floris, F.; Persico, M.; Tani, A.; Tomasi, J. *Chem. Phys.* **1995**, *195*, 207. (c) Sanchez-Marcos, E.; Pappalardo, R. R.; Rinaldi, D. *J. Phys. Chem. A* **1991**, *95*, 8928.

(9) (a) Chaussedent, S.; Monteil, A. *J. Chem. Phys.* **1996**, *105*, 6532. (b) Galera, S.; Lluch, J. M.; Oliva, A.; Bertràn, J.; Foglia, F.; Helm, L.; Merbach, A. *New J. Chem.* **1993**, *17*, 773. (c) Meier, W.; Bopp, Ph.; Probst, M. M.; Spohr, E.; Lin, J. L. *J. Phys. Chem.* **1990**, *94*, 4672.

(10) Kowall, Th.; Foglia, F.; Helm, L.; Merbach, A. *J. Am. Chem. Soc.* **1995**, *117*, 3790.

(11) Gerkin, R. E.; Reppart, W. J. *Acta Crystallogr.* **1984**, *C40*, 781.

(12) Chatterjee, A.; Maslen, E. N.; Watson, K. J. *Acta Crystallogr.* **1988**, *B44*, 381.

(13) (a) Albertsson, J.; Elding, I. *Acta Crystallogr.* **1977**, *B33*, 1460. (b) Sikka, S. K. *Acta Crystallogr.* **1969**, *A25*, 621. (c) Helmholz, L. *J. Am. Chem. Soc.* **1939**, *61*, 1544.

(14) (a) Helm, L.; Merbach, A. *Coord. Chem. Rev.* **1999**, *187*, 151. (b) Cossy, C.; Helm, L.; Powell, D. H.; Merbach, A. E. *New J. Chem.* **1995**, *19*, 27. (c) Ohtaki, H.; Radnai, T. *Chem. Rev.* **1993**, *93*, 1157. (d) Yamaguchi, T.; Nomura, M.; Wakita, H.; Ohtaki, H. *J. Chem. Phys.* **1988**, *89*, 5153.

(15) Dolg, M.; Stoll, H.; Savin, A.; Preuss, H. *Theor. Chim. Acta* **1989**, *75*, 173.

(16) Klamt, A.; Schüürmann, G. *J. Chem. Soc. Perkin Trans.* **1993**, *2*, 799.

(17) Barone, V.; Cossi, M. *J. Phys. Chem. A* **1998**, *102*, 1995.

(18) Cossi, M.; Barone, V. *J. Chem. Phys.* **1998**, *109*, 6246.

(19) Gaussian 98, Revision A.7; Frisch, M. J.; Trucks, G. W.; Schlegel, H. B.; Scuseria, G. E.; Robb, M. A.; Cheeseman, J. R.; Zakrzewski, V. G.; Montgomery, J. A., Jr.; Stratmann, R. E.; Burant, J. C.; Dapprich, S.; Millam, J. M.; Daniels, A. D.; Kudin, K. N.; Strain, M. C.; Farkas, O.; Tomasi, J.; Barone, V.; Cossi, M.; Cammi, R.; Mennucci, B.; Pomelli, C.; Adamo, C.; Clifford, S.; Ochterski, J.; Petersson, G. A.; Ayala, P. Y.; Cui, Q.; Morokuma, K.; Malick, D. K.; Rabuck, A. D.; Raghavachari, K.; Foresman,

J. B.; Cioslowski, J.; Ortiz, J. V.; Stefanov, B. B.; Liu, G.; Liashenko, A.; Piskorz, P.; Komaromi, I.; Gomperts, R.; Martin, R. L.; Fox, D. J.; Keith, T.; Al-Laham, M. A.; Peng, C. Y.; Nanayakkara, A.; Gonzalez, C.; Challacombe, M.; Gill, P. M. W.; Johnson, B.; Chen, W.; Wong, M. W.; Andres, J. L.; Gonzalez, C.; Head-Gordon, M.; Replogle, E. S.; Pople, J. A. Gaussian, Inc.: Pittsburgh, PA, 1998.

(20) Description of the basis sets and explanation of standard levels of theory can be found in: Foresman, J. B.; Frisch, A. e. *Exploring Chemistry with Electronic Structure Methods*, 2nd ed.; Gaussian Inc.: Pittsburgh, PA, 1996.

(21) Adamo, C.; Barone, V. *J. Chem. Phys.* **1998**, *108*, 627.

(22) The experimental absolute hydration free energies for lanthanides, $\Delta G°_{hyd}(Ln^{3+})$,[23] are based on the $\Delta G°_{hyd}(H^+)$ value, the absolute hydration free energy of the H^+ ion, equal to -254.8 kcal mol^{-1}.[24] Recently,[25] a more accurate $\Delta G°_{hyd}(H^+)$ value has been determined (-264.0 kcal mol^{-1}) and, on the basis of this result, the solvation parameters for monatomic ions have been reviewed,[26] leading to a considerably more negative absolute scale than the previously one. Thus, according to ref 26, the absolute $\Delta G°_{hyd}$ values for lanthanides have been updated as follows: $\Delta G°_{hyd}$ $(Ln^{3+}) = \Delta G°_{hyd}$ (Ln^{3+}) [in ref 23] + 3(-254.8) − 3(-264.0).

(23) (a) Guillaumont, D. F. *Radiochem. Radioanal. Lett.* **1974**, *17*, 25. (b) *Gmelin Handbook der Anorganische Chemie, Seltenerdelemente, Teil B7*; Springer: Berlin, 1976.

(24) Conway, B. E. *J. Sol. Chem.* **1978**, *7*, 721.

(25) Tissandier, M. C.; Cowen, K. A.; Feng, W. Y.; Gundlach, E.; Cohen, M. H.; Earhart, A. D.; Coe, J. V.; Tuttle, Jr., T. R. *J. Phys. Chem. A* **1998**, *102*, 7787.

(26) Fawcett, W. R. *J. Phys. Chem. B* **1999**, *103*, 11181.

(27) Shannon, R. *Acta Crystallogr*. **1976**, *A32*, 751.

(28) In vacuo optimizations started from the C_4 and the C_1 geometries of the (Ln-**8**) species converged to S_8 structures, that are confirmed as minima for both the ions by frequency analyses. In the case of the (Ln-**9**) species, the D_3 optimized geometries are characterized as minima by frequency analysis. The C_{3h} and D_{3h} optimized structures correspond to third- and fourth-order saddle points, respectively, 4.9 and 6.3 kcal mol^{-1} for Nd, and 5.5 and 7.2 for Yb kcal mol^{-1} above the D_3 minima. These results are consistent with those previously obtained[2] on the $[Gd(H_2O)_9]^{3+}$ system and confirm the hypothesis that intermolecular interactions, such as crystal packing forces and hydrogen bond networks, should be responsible for the energy stabilization of the C_{3h} and D_{3h} structures of these systems in the solid state. In solution, optimized structures of (Ln-**8**) present S_8 pseudosymmetry; those of (Ln-**9**) show D_3 pseudosymmetry.

(29) Wallqvist, A.; Mountain, R. D. *Rev. Comput. Chem.*; Lipkowitz, K. B., Boyd D. B., Eds.; Wiley-VCH: New York, 1999; Vol. 13, Chapter 4: "Molecular Models of Water: Derivation and Description" and references within.